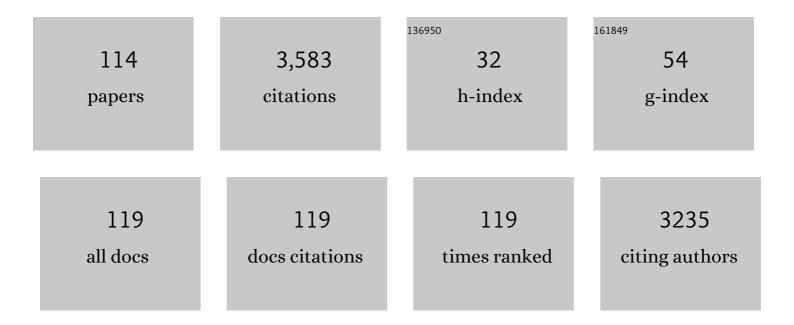
List of Publications by Year in descending order

Source: https://exaly.com/author-pdf/4506196/publications.pdf Version: 2024-02-01



#	Article	IF	CITATIONS
1	Imaging Pituitary Vasopressin 1B Receptor in Humans with the PET Radiotracer ¹¹ C-TASP699. Journal of Nuclear Medicine, 2022, 63, 609-614.	5.0	7
2	Association of entorhinal cortical tau deposition and hippocampal synaptic density in older individuals with normal cognition and early Alzheimer's disease. Neurobiology of Aging, 2022, 111, 44-53.	3.1	25
3	Lower prefrontal cortical synaptic vesicle binding in cocaine use disorder: An exploratory ¹¹ Câ€UCBâ€J positron emission tomography study in humans. Addiction Biology, 2022, 27, e13123.	2.6	16
4	Synaptic density and cognitive performance in Alzheimer's disease: A PET imaging study with [¹¹ C]UCBâ€J. Alzheimer's and Dementia, 2022, 18, 2527-2536.	0.8	55
5	Imaging the effect of ketamine on synaptic density (SV2A) in the living brain. Molecular Psychiatry, 2022, 27, 2273-2281.	7.9	25
6	Adaptive data-driven motion detection and optimized correction for brain PET. NeuroImage, 2022, 252, 119031.	4.2	8
7	Brain opioid segments and striatal patterns of dopamine release induced by naloxone and morphine. Human Brain Mapping, 2022, 43, 1419-1430.	3.6	11
8	lmaging of Synaptic Density in Neurodegenerative Disorders. Journal of Nuclear Medicine, 2022, 63, 60S-67S.	5.0	29
9	Preliminary in vivo evidence of lower hippocampal synaptic density in cannabis use disorder. Molecular Psychiatry, 2021, 26, 3192-3200.	7.9	32
10	Simplified Quantification of ¹¹ C-UCB-J PET Evaluated in a Large Human Cohort. Journal of Nuclear Medicine, 2021, 62, 418-421.	5.0	19
11	First-in-Human Evaluation of ¹⁸ F-SynVesT-1, a Radioligand for PET Imaging of Synaptic Vesicle Glycoprotein 2A. Journal of Nuclear Medicine, 2021, 62, 561-567.	5.0	60
12	First-in-Human Assessment of ¹¹ C-LSN3172176, an M1 Muscarinic Acetylcholine Receptor PET Radiotracer. Journal of Nuclear Medicine, 2021, 62, 553-560.	5.0	35
13	PET Imaging Estimates of Regional Acetylcholine Concentration Variation in Living Human Brain. Cerebral Cortex, 2021, 31, 2787-2798.	2.9	5
14	Association of Aβ deposition and regional synaptic density in early Alzheimer's disease: a PET imaging study with [11C]UCB-J. Alzheimer's Research and Therapy, 2021, 13, 11.	6.2	53
15	Assessment of test-retest reproducibility of [18F]SynVesT-1, a novel radiotracer for PET imaging of synaptic vesicle glycoprotein 2A. European Journal of Nuclear Medicine and Molecular Imaging, 2021, 48, 1327-1338.	6.4	23
16	Comparison of [¹¹ C]UCB-J and [¹⁸ F]FDG PET in Alzheimer's disease: A tracer kinetic modeling study. Journal of Cerebral Blood Flow and Metabolism, 2021, 41, 2395-2409.	4.3	43
17	Synaptic density is associated with cognitive performance in early Alzheimer's disease: a PET imaging study with [11C]UCB-J. American Journal of Geriatric Psychiatry, 2021, 29, S119-S120.	1.2	1
18	Principal component analysis of synaptic density measured with [11C]UCB-J PET in Alzheimer's disease. American Journal of Geriatric Psychiatry, 2021, 29, S47-S48.	1.2	0

#	Article	IF	CITATIONS
19	Preliminary In Vivo Evidence of Reduced Synaptic Density in Human Immunodeficiency Virus (HIV) Despite Antiretroviral Therapy. Clinical Infectious Diseases, 2021, 73, 1404-1411.	5.8	25
20	Imaging the Effect of Ketamine on Synaptic (SV2A) Density. Biological Psychiatry, 2021, 89, S35.	1.3	0
21	In vivo evidence of lower synaptic vesicle density in schizophrenia. Molecular Psychiatry, 2021, 26, 7690-7698.	7.9	51
22	Generation of synthetic PET images of synaptic density and amyloid from ¹⁸ Fâ€FDG images using deep learning. Medical Physics, 2021, 48, 5115-5129.	3.0	12
23	Generation of parametric <i>K</i> _i images for FDG PET using two 5â€min scans. Medical Physics, 2021, 48, 5219-5231.	3.0	16
24	Partial volume correction analysis for 11C-UCB-J PET studies of Alzheimer's disease. NeuroImage, 2021, 238, 118248.	4.2	17
25	PET Imaging of Synaptic Vesicle Protein 2A. , 2021, , 993-1019.		10
26	Parametric Imaging With PET and SPECT. IEEE Transactions on Radiation and Plasma Medical Sciences, 2020, 4, 1-23.	3.7	43
27	PET Imaging of Pancreatic Dopamine D ₂ and D ₃ Receptor Density with ¹¹ C-(+)-PHNO in Type 1 Diabetes. Journal of Nuclear Medicine, 2020, 61, 570-576.	5.0	19
28	Atlas-Based Multiorgan Segmentation for Dynamic Abdominal PET. IEEE Transactions on Radiation and Plasma Medical Sciences, 2020, 4, 50-62.	3.7	14
29	Assessment of a white matter reference region for ¹¹ C-UCB-J PET quantification. Journal of Cerebral Blood Flow and Metabolism, 2020, 40, 1890-1901.	4.3	77
30	Reduced synaptic vesicle protein 2A binding in temporal lobe epilepsy: A [¹¹ C]UCBâ€J positron emission tomography study. Epilepsia, 2020, 61, 2183-2193.	5.1	51
31	In vivo measurement of widespread synaptic loss and associated tau accumulation in early Alzheimer's disease. Alzheimer's and Dementia, 2020, 16, e037791.	0.8	1
32	ICAâ€derived sources of synaptic density PET ([11 C]UCBâ€) relate to cognitive impairment severity in Alzheimer's disease. Alzheimer's and Dementia, 2020, 16, e041197.	0.8	3
33	Association between cerebral amyloid accumulation and synaptic density in Alzheimer's disease: A multitracer PET study. Alzheimer's and Dementia, 2020, 16, e043631.	0.8	0
34	Association between cerebrospinal fluid biomarkers of neurodegeneration and PET measurements of synaptic density in Alzheimer's disease. Alzheimer's and Dementia, 2020, 16, e044211.	0.8	2
35	Validation of a simplified tissueâ€toâ€reference ratio measurement using SUVR for the assessment of synaptic density alterations in Alzheimer's disease using [11 C]UCBâ€J PET. Alzheimer's and Dementia, 2020, 16, e045928.	0.8	1
36	In vivo measurement of widespread synaptic loss in Alzheimer's disease with SV2A PET. Alzheimer's and Dementia, 2020, 16, 974-982.	0.8	170

#	Article	IF	CITATIONS
37	Kinetic Modeling and Test–Retest Reproducibility of ¹¹ C-EKAP and ¹¹ C-FEKAP, Novel Agonist Radiotracers for PET Imaging of the Iº-Opioid Receptor in Humans. Journal of Nuclear Medicine, 2020, 61, 1636-1642.	5.0	10
38	ASSOCIATION BETWEEN CEREBRAL AMYLOID ACCUMULATION AND SYNAPTIC DENSITY IN ALZHEIMER'S DISEASE: A MULTITRACER PET STUDY. American Journal of Geriatric Psychiatry, 2020, 28, S123-S124.	1.2	0
39	Synaptic Changes in Parkinson Disease Assessed with in vivo Imaging. Annals of Neurology, 2020, 87, 329-338.	5.3	112
40	Data-Driven Motion Detection and Event-by-Event Correction for Brain PET: Comparison with Vicra. Journal of Nuclear Medicine, 2020, 61, 1397-1403.	5.0	32
41	Assessment of population-based input functions for Patlak imaging of whole body dynamic 18F-FDG PET. EJNMMI Physics, 2020, 7, 67.	2.7	45
42	S13. IN VIVO EVIDENCE OF REDUCED SYNAPTIC VESICLE DENSITY IN SCHIZOPHRENIA USING [11C] UCB-J PET IMAGING. Schizophrenia Bulletin, 2019, 45, S310-S311.	4.3	0
43	Data-driven voluntary body motion detection and non-rigid event-by-event correction for static and dynamic PET. Physics in Medicine and Biology, 2019, 64, 065002.	3.0	32
44	In Vivo Synaptic Density Imaging with ¹¹ C-UCB-J Detects Treatment Effects of Saracatinib in a Mouse Model of Alzheimer Disease. Journal of Nuclear Medicine, 2019, 60, 1780-1786.	5.0	57
45	142. Synaptic Density Alterations are Associated With Depression Severity and Network Alterations. Biological Psychiatry, 2019, 85, S59.	1.3	4
46	Social status and demographic effects of the kappa opioid receptor: a PET imaging study with a novel agonist radiotracer in healthy volunteers. Neuropsychopharmacology, 2019, 44, 1714-1719.	5.4	22
47	A singleâ€center, openâ€label positron emission tomography study to evaluate brivaracetam and levetiracetam synaptic vesicle glycoprotein 2A binding in healthy volunteers. Epilepsia, 2019, 60, 958-967.	5.1	45
48	Lower synaptic density is associated with depression severity and network alterations. Nature Communications, 2019, 10, 1529.	12.8	277
49	Novel Kappa Opioid Receptor Agonist as Improved PET Radiotracer: Development and in Vivo Evaluation. Molecular Pharmaceutics, 2019, 16, 1523-1531.	4.6	9
50	P4â€481: ASSOCIATION BETWEEN ENTORHINAL CORTICAL TAU ACCUMULATION AND HIPPOCAMPAL SYNAPTIC DENSITY IN OLDER INDIVIDUALS WITH NORMAL COGNITION AND EARLY ALZHEIMER'S DISEASE: PRELIMINARY EXPERIENCE. Alzheimer's and Dementia, 2019, 15, P1497.	0.8	0
51	ICâ€Pâ€140: ASSOCIATION BETWEEN MGLUR5 AND SYNAPTIC DENSITY: A MULTIâ€TRACER STUDY IN HEALTHY A AND ALZHEIMER'S DISEASE. Alzheimer's and Dementia, 2019, 15, P115.	KGING	0
52	Development and In Vivo Evaluation of a κ-Opioid Receptor Agonist as a PET Radiotracer with Superior Imaging Characteristics. Journal of Nuclear Medicine, 2019, 60, 1023-1030.	5.0	20
53	Quantitative PET Imaging in Drug Development: Estimation of Target Occupancy. Bulletin of Mathematical Biology, 2019, 81, 3508-3541.	1.9	21
54	Evaluation of Pancreatic VMAT2 Binding with Active and Inactive Enantiomers of [18F]FP-DTBZ in Healthy Subjects and Patients with Type 1 Diabetes. Molecular Imaging and Biology, 2018, 20, 835-845.	2.6	24

#	Article	IF	CITATIONS
55	Evaluation of PET Brain Radioligands for Imaging Pancreatic β-Cell Mass: Potential Utility of 11C-(+)-PHNO. Journal of Nuclear Medicine, 2018, 59, 1249-1254.	5.0	22
56	Dose-Related Target Occupancy and Effects on Circuitry, Behavior, and Neuroplasticity of the Glycine Transporter-1 Inhibitor PF-03463275 in Healthy and Schizophrenia Subjects. Biological Psychiatry, 2018, 84, 413-421.	1.3	43
57	Decreased VMAT2 in the pancreas of humans with type 2 diabetes mellitus measured in vivo by PET imaging. Diabetologia, 2018, 61, 2598-2607.	6.3	18
58	Novel ¹⁸ F-Labeled κ-Opioid Receptor Antagonist as PET Radiotracer: Synthesis and In Vivo Evaluation of ¹⁸ F-LY2459989 in Nonhuman Primates. Journal of Nuclear Medicine, 2018, 59, 140-146.	5.0	28
59	P2â€365: PET IMAGING OF SYNAPTIC DENSITY (SYNAPTIC VESICLE GLYCOPROTEIN 2A, SV2A) IN ALZHEIMER'S DISEASE: INITIAL EXPERIENCE. Alzheimer's and Dementia, 2018, 14, P832.	0.8	0
60	ICâ€Pâ€183: PET IMAGING OF SYNAPTIC DENSITY (SYNAPTIC VESICLE GLYCOPROTEIN 2A, SV2A) IN ALZHEIMER'S DISEASE: INITIAL EXPERIENCE. Alzheimer's and Dementia, 2018, 14, P152.	0.8	0
61	Initial Experience with PET Imaging of Synaptic Density (SV2A) in Alzheimer's Disease: A New Biomarker for Clinical Trials?. American Journal of Geriatric Psychiatry, 2018, 26, S145-S146.	1.2	3
62	F149. Preliminary Evidence for Altered Synaptic Density and a Possible Role for Accelerated Ageing in Individuals With MDD as Measured With [11C]UCB-J PET. Biological Psychiatry, 2018, 83, S296.	1.3	4
63	Assessing Synaptic Density in Alzheimer Disease With Synaptic Vesicle Glycoprotein 2A Positron Emission Tomographic Imaging. JAMA Neurology, 2018, 75, 1215.	9.0	304
64	Improved discrimination between benign and malignant LDCT screening-detected lung nodules with dynamic over static ¹⁸ F-FDG PET as a function of injected dose. Physics in Medicine and Biology, 2018, 63, 175015.	3.0	17
65	Comparative evaluation of two glycine transporter 1 radiotracers [11C]GSK931145 and [18F]MK-6577 in baboons. Synapse, 2016, 70, 112-120.	1.2	4
66	Preclinical Evaluation of ¹⁸ F-PF-05270430, a Novel PET Radioligand for the Phosphodiesterase 2A Enzyme. Journal of Nuclear Medicine, 2016, 57, 1448-1453.	5.0	13
67	Event-by-Event Continuous Respiratory Motion Correction for Dynamic PET Imaging. Journal of Nuclear Medicine, 2016, 57, 1084-1090.	5.0	39
68	First-in-Human Assessment of the Novel PDE2A PET Radiotracer ¹⁸ F-PF-05270430. Journal of Nuclear Medicine, 2016, 57, 1388-1395.	5.0	27
69	Evaluation of pancreatic VMAT2 binding with active and inactive enantiomers of 18 F-FP-DTBZ in baboons. Nuclear Medicine and Biology, 2016, 43, 743-751.	0.6	20
70	Receptor Occupancy of the Â-Opioid Antagonist LY2456302 Measured with Positron Emission Tomography and the Novel Radiotracer 11C-LY2795050. Journal of Pharmacology and Experimental Therapeutics, 2016, 356, 260-266.	2.5	47
71	Test–Retest Reproducibility of Binding Parameters in Humans with ¹¹ C-LY2795050, an Antagonist PET Radiotracer for the κ Opioid Receptor. Journal of Nuclear Medicine, 2015, 56, 243-248.	5.0	35
72	Test-retest variability of adenosine A2A binding in the human brain with 11C-TMSX and PET. EJNMMI Research, 2014, 4, 76.	2.5	13

#	Article	IF	CITATIONS
73	Association of In Vivo κ-Opioid Receptor Availability and the Transdiagnostic Dimensional Expression of Trauma-Related Psychopathology. JAMA Psychiatry, 2014, 71, 1262.	11.0	67
74	Kinetic Modeling of 11C-LY2795050, A Novel Antagonist Radiotracer for PET Imaging of the Kappa Opioid Receptor in Humans. Journal of Cerebral Blood Flow and Metabolism, 2014, 34, 1818-1825.	4.3	42
75	Clinical doses of atomoxetine significantly occupy both norepinephrine and serotonin transports: Implications on treatment of depression and ADHD. NeuroImage, 2014, 86, 164-171.	4.2	75
76	Evaluation of the agonist PET radioligand [11C]GR103545 to image kappa opioid receptor in humans: Kinetic model selection, test–retest reproducibility and receptor occupancy by the antagonist PF-04455242. NeuroImage, 2014, 99, 69-79.	4.2	54
77	Eventâ€byâ€event respiratory motion correction for PET with 3D internalâ€1D external motion correlation. Medical Physics, 2013, 40, 112507.	3.0	27
78	Tracer Kinetic Modeling of [¹¹ C]AFM, a New PET Imaging Agent for the Serotonin Transporter. Journal of Cerebral Blood Flow and Metabolism, 2013, 33, 1886-1896.	4.3	17
79	Event-by-event respiratory motion correction for PET with 3-Dimensional internal-external motion correlation. , 2012, , .		5
80	Brain tissue selection procedures for image derived input functions derived using independent components analysis. , 2012, 2012, 5987-90.		1
81	Quantification of Neuroreceptors and Neurotransporters. Neuromethods, 2012, , 149-161.	0.3	1
82	Differential effects of age on human striatal adenosine A ₁ and A _{2A} receptors. Synapse, 2012, 66, 832-839.	1.2	18
83	Adenosine A2A Receptors Measured with [11C]TMSX PET in the Striata of Parkinson's Disease Patients. PLoS ONE, 2011, 6, e17338.	2.5	122
84	Imaging of I2-imidazoline receptors by small-animal PET using 2-(3-fluoro-[4-11C]tolyl)-4,5-dihydro-1H-imidazole ([11C]FTIMD). Nuclear Medicine and Biology, 2010, 37, 625-635.	0.6	28
85	A new graphic plot analysis for determination of neuroreceptor binding in positron emission tomography studies. Neurolmage, 2010, 49, 578-586.	4.2	8
86	Improvement of likelihood estimation in Logan graphical analysis using maximum a posteriori for neuroreceptor PET imaging. Annals of Nuclear Medicine, 2009, 23, 163-171.	2.2	8
87	Wavelet denoising for voxel-based compartmental analysis of peripheral benzodiazepine receptors with 18F-FEDAA1106. European Journal of Nuclear Medicine and Molecular Imaging, 2008, 35, 416-423.	6.4	15
88	PET kinetic analysis: error consideration of quantitative analysis in dynamic studies. Annals of Nuclear Medicine, 2008, 22, 1-11.	2.2	28
89	Shortened protocol in practical [11C]SA4503-PET studies for sigma1 receptor quantification. Annals of Nuclear Medicine, 2008, 22, 143-146.	2.2	13
90	Robust estimation of the arterial input function for Logan plots using an intersectional searching algorithm and clustering in positron emission tomography for neuroreceptor imaging. Neurolmage, 2008, 40, 26-34.	4.2	19

#	Article	IF	CITATIONS
91	Reduction of noise-induced underestimation in Logan graphical analysis using scale invariant linear estimation. NeuroImage, 2008, 41, T82.	4.2	0
92	Parametric Imaging of the total volume of distribution using MAP estimation for logan graphical analysis. NeuroImage, 2008, 41, T83.	4.2	1
93	Mapping of human cerebral sigma1 receptors using positron emission tomography and [11C]SA4503. NeuroImage, 2007, 35, 1-8.	4.2	56
94	Omission of serial arterial blood sampling for quantitative analysis of monkey PET data using independent component analysis-based method. , 2007, , .		3
95	High Occupancy of Sigma-1 Receptors in the Human Brain after Single Oral Administration of Fluvoxamine: A Positron Emission Tomography Study Using [11C]SA4503. Biological Psychiatry, 2007, 62, 878-883.	1.3	122
96	Temporal and spatial blood information estimation using Bayesian ICA in dynamic cerebral positron emission tomography. , 2007, 17, 979-993.		7
97	Evaluation of distribution of adenosine A2A receptors in normal human brain measured with [11C]TMSX PET. Synapse, 2007, 61, 778-784.	1.2	67
98	PET kinetic analysis —Pitfalls and a solution for the Logan plot. Annals of Nuclear Medicine, 2007, 21, 1-8.	2.2	39
99	Quantification of adenosine A2A receptors in the human brain using [11C]TMSX and positron emission tomography. European Journal of Nuclear Medicine and Molecular Imaging, 2007, 34, 679-687.	6.4	30
100	PET kinetic analysis: wavelet denoising of dynamic PET data with application to parametric imaging. Annals of Nuclear Medicine, 2007, 21, 379-386.	2.2	31
101	Distribution volume as an alternative to the binding potential for sigma1 receptor imaging. Annals of Nuclear Medicine, 2007, 21, 533-535.	2.2	17
102	Whole Shape Measurement System Using a Single Camera and a Cylindrical Mirror. , 2006, , .		1
103	MAP-based kinetic analysis for voxel-by-voxel compartment model estimation: Detailed imaging of the cerebral glucose metabolism using FDG. NeuroImage, 2006, 29, 1203-1211.	4.2	11
104	PET kinetic analysis—compartmental model. Annals of Nuclear Medicine, 2006, 20, 583-588.	2.2	164
105	A feasibility study of [11C]SA4503-PET for evaluating sigma1 receptor occupancy by neuroleptics: The binding of haloperidol to sigma1 and dopamine D2-like receptors. Annals of Nuclear Medicine, 2006, 20, 569-573.	2.2	33
106	Extraction of a Plasma Time-Activity Curve From Dynamic Brain PET Images Based on Independent Component Analysis. IEEE Transactions on Biomedical Engineering, 2005, 52, 201-210.	4.2	107
107	Imaging detailed glucose metabolism in the brain using MAP estimation in Positron Emission Tomography. , 2005, 2005, 4477-9.		1
108	3D Imaging System for Visualizing and Monitoring Patients. , 2005, 2005, 3735-7.		0

7

#	Article	IF	CITATIONS
109	Practical Consideration about Cost Functions of Spatial Independent Component Analysis in Medical Image Processing. , 2005, 2005, 1120-2.		1
110	Omission of serial arterial blood sampling in neuroreceptor imaging with independent component analysis. NeuroImage, 2005, 26, 885-890.	4.2	29
111	Doctor-to-Patient communication by 2.5G mobile phone; preliminary study. International Congress Series, 2005, 1281, 196-199.	0.2	4
112	Formation of binding potential maps of adenosine A1 and A2A receptors using independent component analysis without arterial blood sampling. Journal of Cerebral Blood Flow and Metabolism, 2005, 25, S606-S606.	4.3	1
113	Three-Dimensional Measurement System Using a Cylindrical Mirror. Lecture Notes in Computer Science, 2005, , 399-408.	1.3	1
114	Clustering approach for voxel-based Logan plot to improve noise reduction capability. Journal of Cerebral Blood Flow and Metabolism, 2005, 25, S632-S632.	4.3	1